Contract No:

This document was prepared in conjunction with work accomplished under Contract No. DE-AC09-08SR22470 with the U.S. Department of Energy (DOE) Office of Environmental Management (EM).

Disclaimer:

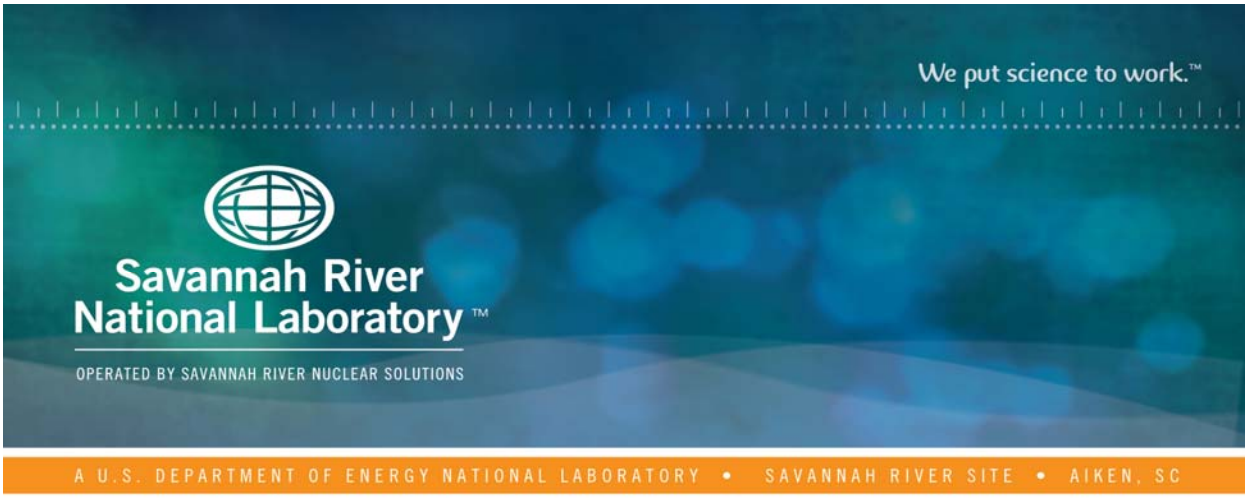

Radiolytic and Thermolytic Bubble Gas Hydrogen Composition

W. H. Woodham

December 2017

SRNL-STI-2017-00593, Revision 0

DISCLAIMER

Printed in the United States of America

Prepared for
U.S. Department of Energy

SRNL-STI-2017-00593
Revision 0

Keywords: *Hydrogen, Radiolysis, Thermolysis*

Retention: *Permanent*

Radiolytic and Thermolytic Bubble Gas Hydrogen Composition

W. H. Woodham

December 2017

Prepared for the U.S. Department of Energy under contract number DE-AC09-08SR22470.

Savannah River National Laboratory™
OPERATED BY SAVANNAH RIVER NUCLEAR SOLUTIONS

REVIEWS AND APPROVALS

AUTHORS:

W. H. Woodham, Process Technology Programs Date

TECHNICAL REVIEW:

C. L. Crawford, Advanced Characterization and Processing, Reviewed per E7 2.60 Date

APPROVAL:

F. M. Pennebaker, Chemical Processing Technologies Date

D. E. Dooley, Manager Date
Chemical Processing Technologies

R. E. Edwards, Manager Date
Nuclear Safety & Engineering Integration, Savannah River Remediation

E. J. Freed, Manager Date
DWPF/Saltstone Facility Engineering, Savannah River Remediation

J. P. Schwenker, Jr., Manager Date
Tank Farm Facility Engineering, Savannah River Remediation

EXECUTIVE SUMMARY

This report describes the development of a mathematical model for the estimation of the hydrogen composition of gas bubbles trapped in radioactive waste. The model described herein uses a material balance approach to accurately incorporate the rates of hydrogen generation by a number of physical phenomena and scale the aforementioned rates in a manner that allows calculation of the final hydrogen composition. The proposed model accounts for the following physical phenomena:

- H_2 generation by primary radiolysis of water and salt solutions
- H_2 generation by secondary radiolysis of formate and glycolate molecules in solution
- Negligible H_2 generation by thermolysis of formate at temperatures below 120 °C
- H_2 generation by thermolysis of glycolate in caustic solutions
- O_2 consumption by radiolyzed and thermolyzed organic species

Additionally, the proposed model conservatively excludes a number of physical phenomena that are known to contribute slightly to the hydrogen composition in trapped gas bubbles:

- Equilibrium concentration of water vapor in trapped gas bubbles
- Generation of N_2O during radiolysis of nitrite solutions
- Incomplete consumption of O_2 by organics

The following conclusions may be made concerning the model described:

- Improvements have been made to more accurately describe the effects of nitrate and nitrite salts on the hydrogen composition of gas generated from salt solution radiolysis. Previously unused literature data has been evaluated and used to improve the prediction of nitrate effects, prompting the recommendation of an inverse-linear fit to reported data (as opposed to the cubic fit currently employed).
- The method described by Crawford and King[1] for calculating the hydrogen generation rate from the radiolysis of formate and glycolate has been incorporated. It is an assumption of the model that the effect of organic radiolysis on hydrogen composition is strictly additive in that only H_2 is released as a gaseous product.
- The method described by Crawford and King[1] for calculating the hydrogen generation rate from the thermolysis of glycolate has been incorporated. This was accomplished with the use of vapor-phase compositional data provided by Ashby.[2] It was shown that the effect of glycolate thermolysis on hydrogen composition is not strictly additive due to the tendency of glycolate to form additional gases (N_2, N_2O, etc.) upon thermolysis. It was also suggested that formate thermolysis is negligible at the applicable conditions.
- A bounding technique for approximating the effect of oxygen consumption by formate and glycolate has been developed and applied to the model described. The approximation determines the upper bound of oxygen consumption by comparing the rate of organic byproduct formation by organic radiolysis and thermolysis to the rate of oxygen generation by salt solution radiolysis. It was shown that the effect of this approximation on hydrogen composition is strictly additive due to the selective removal of O_2 from the trapped gas vapor phase.
- Using a sample calculation case with the same nitrate and nitrite concentrations used in a previous treatment of H_{mix}, this work finds:
    - H_2 generation by primary radiolysis of water and salt solutions, $H_{mix} = 0.141$
    - H_2 generation by secondary radiolysis of formate and glycolate molecules in solution, $H_{mix} = 0.169$

- H_2 generation by thermolysis of glycolate in caustic solutions, $H_{mix} = 0.160$
- O_2 consumption by radiolyzed and thermolyzed organic species, $H_{mix} = 0.184$

The hydrogen composition model described in this report is recommended as an improvement over existing calculation methods due to the models realistic treatment of nitrate effects on hydrogen composition and inclusion of format and glycolate radiolytic and thermolytic effects. In order to generated a bounding model for use with all organics present in SRS liquid waste, the following recommendations are made to generate data for the improvement of the model:

- Real-waste and simulant testing should be performed such that the accuracy of the predictions made by this model can be confirmed. In particular, the recommended testing should examine the production rates of H_2, N_2O, N_2, and any other gases evolved from radioactive waste at caustic conditions. If practical, this testing should be designed with sufficient sensitivity to allow for the determination of oxygen consumption.
- Additional testing should be performed to evaluate the validity of this model with regards to the multitude of organic species known to exist in Savannah River Site (SRS) waste streams (e.g., tributylphosphate, Isopar^{TM}, etc.). Focus should be given to understanding the composition of vapors produced by organic radiolysis and thermolysis as a function of both temperature and organic speciation. Such data may be coupled with the thermolytic model developed by Hu[3] in order to generate a comprehensive hydrogen composition model for trapped gas bubbles in radioactive waste.

TABLE OF CONTENTS

LIST OF TABLES

LIST OF FIGURES

LIST OF ABBREVIATIONS

BF-EXP	Best-Fit Exponential (model for nitrate radiolysis)
BF-INV	Best-Fit Inverse (model for nitrate radiolysis)
C-EXP	Conservative Exponential (model for nitrate radiolysis)
C-INV	Conservative Inverse (model for nitrate radiolysis)
CPC	Chemical Process Cell
DWPF	Defense Waste Processing Facility
HGR	Hydrogen Generation Rate
PISA	Potential Inadequacy in the Safety Analysis
SRNL	Savannah River National Laboratory
SRR	Savannah River Remediation
SRS	Savannah River Site
TTR	Technical Task Request

1.0 Introduction

Savannah River Remediation (SRR) personnel have requested that Savannah River National Laboratory (SRNL) researchers evaluate potential impacts of glycolate on Savannah River Site (SRS) Tank Farm flammability calculations.[4,5] These calculations include the generation rate of hydrogen due to glycolate radiolysis and thermolysis as well as the contribution of glycolate to the hydrogen composition of trapped gas bubbles in radioactive liquid waste. In addition to this request, SRR personnel have requested that SRNL researchers evaluate similar potential impacts from formate in response to three Potential Inadequacies in the Safety Analyses (PISAs) concerning the unaddressed impacts of hydrogen generation from organic molecules in the Tank Farm[6], DWPF[7], and Saltstone facilities[8]. Currently, glycolate is not present in SRS Tank Farm waste in large amounts, but is expected to be introduced with the implementation of the alternate reductant flowsheet[9] in the Defense Waste Processing Facility (DWPF). Formate ion is already present in SRS Tank Farm waste at levels greater than 2 g/L,[10] introduced primarily by DWPF as a reducing agent (formic acid) for waste treatment in the Chemical Process Cell (CPC).[11]

The evaluation of formate and glycolate impacts on Hydrogen Generation Rate (HGR) has already been evaluated by Crawford and King.[1] Literature data for reaction rate constants were used to develop a methodology for estimating the amount of hydrogen gas generated by secondary radiolysis of formate and glycolate, and experimental results by Ashby *et al.*[2] were used to generate a reaction rate model for the thermolytic degradation of glycolate to form hydrogen gas. The purpose of this report is to document the use of the methods developed by Crawford and King as well as additional literature data to develop a mathematical model for the prediction of trapped bubble hydrogen composition to potentially replace the existing methodology[12], thereby completing the Task #2 and Deliverable #3 items identified in the Technical Task Request (TTR)[4].

2.0 Summary of Calculation Method

2.1 Calculation Overview

The hydrogen composition of gases trapped in radioactive waste may be approximated by accounting for every gaseous generation mechanism in terms of a material balance. With knowledge of the total amounts of gases produced as well as the hydrogen fraction of each gas production mechanism, one may predict the hydrogen composition by the following equation (Equation [1]):

$$H_{mix} = \frac{\sum y_{H_2}^{i} \dot{n}_i}{\sum \dot{n}_i} \qquad [1]$$

where H_{mix} is the mole fraction of hydrogen in the trapped vapor phase, $y_{H_2}^{i}$ is the mole fraction of hydrogen present in the gas produced from production mechanism "i", and $\dot{n}_i$ is the molar production rate of total gas from production mechanism "i".

When considering the composition of hydrogen in organic-containing radioactive waste, several gas production mechanisms exist that should be evaluated. Such mechanisms include primary and secondary radiolysis of water/salt solutions, secondary radiolysis of organic molecules, thermolysis of organic molecules, and oxygen depletion by organics. For the purposes of this report, only glycolate and formate will be considered as organic contributors to hydrogen composition. Additionally, only radiolytic and thermolytic generation mechanisms will be evaluated: corrosion is expected to be negligible in the presence of nitrite and nitrate salts.[13] It is important to note that although oxygen depletion by organics does not produce additional hydrogen gas, it does decrease the amount of oxygen present in the trapped gas bubble,

which in turn increases the relative concentrations of hydrogen in trapped gas (CO_2, formed by oxidation of organic molecules, will be absorbed by caustic solutions, and will therefore not factor into the calculation of vapor phase concentrations).

Equation [1] may be re-written in terms of the mechanisms described above in order to generate a useful equation for the calculation of hydrogen composition. This modified equation is given below in Equation [2]:

$$H_{mix} = \frac{y_w^r \dot{n}_w^r + y_g^r \dot{n}_g^r + y_f^r \dot{n}_f^r + y_g^t \dot{n}_g^t + y_f^t \dot{n}_f^t}{\dot{n}_w^r + \dot{n}_g^r + \dot{n}_f^r + \dot{n}_g^t + \dot{n}_f^t - \dot{n}_{OD}} \quad [2]$$

where "y"s are hydrogen mole fractions, "n"s are total gas molar production rates, subscript "w", "g", and "f" refer to "water", "glycolate", and "formate" production mechanisms, respectively, and superscript "r" and "t" refer to "radiolytic" and "thermolytic" production mechanisms, respectively. $\dot{n}_{OD}$ refers to the molar consumption rate of oxygen depletion caused by organics in the waste. Each of these mechanisms are described in detail in sections 2.2 through 2.5.

2.2 Effects of Nitrate and Nitrite on Bubble Compositions

A method for calculating the hydrogen fraction of gases produced from salt solution radiolysis has been previously described by Hester.[12] The technique uses the concentrations of nitrite and nitrate salts in solution to account for the ability of these salts to hinder the production of H_2 according to the following equations:

$$y_w^r = H_{NO_3} F_{NO_3} C_{NO_3} + H_{NO_2} F_{NO_2} C_{NO_2} \quad [3]$$

$$H_{NO_3} = 0.0242[NO_3]^3 - 0.076[NO_3]^2 - 0.2101[NO_3] + 0.69 \quad [4]$$

$$H_{NO_2}([NO_2] < 1M) = 1.0213[NO_2]^2 - 1.2235[NO_2] + 0.9821 \quad [5]$$

$$H_{NO_2}([NO_2] \geq 1M) = 0.035[NO_2] + 0.74 \quad [6]$$

$$F_{NO_3} = \frac{[NO_3]}{[NO_2] + [NO_3]} \quad [7]$$

$$F_{NO_2} = \frac{[NO_2]}{[NO_2] + [NO_3]} \quad [8]$$

$$C_{NO_3} = \frac{\omega_\alpha G_\alpha(H_2)\big|^{NO_2,NO_3} + \omega_{\beta/\gamma} G_{\beta/\gamma}(H_2)\big|^{NO_2,NO_3}}{\omega_\alpha G_\alpha(H_2)\big|^{0,NO_3} + \omega_{\beta/\gamma} G_{\beta/\gamma}(H_2)\big|^{0,NO_3}} \quad [9]$$

$$C_{NO_2} = \frac{\omega_\alpha G_\alpha(H_2)\big|^{NO_2,NO_3} + \omega_{\beta/\gamma} G_{\beta/\gamma}(H_2)\big|^{NO_2,NO_3}}{\omega_\alpha G_\alpha(H_2)\big|^{NO_2,0} + \omega_{\beta/\gamma} G_{\beta/\gamma}(H_2)\big|^{NO_2,0}} \quad [10]$$

$$G_{\alpha}\left(H_2\right)\Big|^{NO_2,NO_3} = 1.3 - 0.79\left[NO_{eff}\Big|^{NO_2,NO_3}\right]^{1/3} - 0.13\left[NO_{eff}\Big|^{NO_2,NO_3}\right]^{2/3} + 0.11\left[NO_{eff}\Big|^{NO_2,NO_3}\right] \quad [11]$$

$$G_{\beta/\gamma}\left(H_2\right)\Big|^{NO_2,NO_3} = 0.466 - 0.51\left[NO_{eff}\Big|^{NO_2,NO_3}\right]^{1/3} + 0.14\left[NO_{eff}\Big|^{NO_2,NO_3}\right]^{2/3} + 0.0055\left[NO_{eff}\Big|^{NO_2,NO_3}\right] \quad [12]$$

$$\left[NO_{eff}\Big|^{NO_2,NO_3}\right] = \left[NO_3\right] + \tfrac{1}{2}\left[NO_2\right] \quad [13]$$

where $\left[NO_3\right]$ is the concentration of nitrate, $\left[NO_2\right]$ is the concentration of nitrite, ω_{α} is the fraction of absorbed radiation heat due to alpha decay, and $\omega_{\beta/\gamma}$ is the fraction of absorbed radiation heat due to beta and gamma decay.

It has been suggested that the curve fits used to develop Equations [4] through [6] are suboptimal, leading to significant overpredictions of hydrogen composition at nitrate concentrations larger than 4 M and slight underpredictions at concentrations between 2 and 4 M. Improved curve fits are discussed later in this report.

Molar production rates of H_2 from salt solution radiolysis have been previously described by Boley[14], and are captured in Equations [11] and [12]. Using the molar production rates and mole fraction of H_2, the total gas production from salt solution radiolysis may be calculated according to Equation [14]:

$$\dot{n}_w^r = \frac{\dot{n}_{H_2,w}^r}{y_w^r} \quad [14]$$

where $\dot{n}_{H_2,w}^r$ is the molar production rate of H_2 from salt solution radiolysis, described in Equations [11] and [12]. Note that this term refers to a production rate based on moles of H_2 released per radiative energy absorbed: any mass-based measurement of H_2 would, by definition, require a conversion factor involving radiative heat for Equations [11], [12], and [14] to be used to calculate a hydrogen generation rate.

2.3 Effects of Organic Radiolysis on Bubble Compositions

Crawford and King[1] have recently reported a method to predict the hydrogen generation from radiolysis of formate and glycolate using the competition kinetics calculation described by Bibler *et al.*[15] This method calculates the rate of hydrogen formation by multiplying the relative reactivities of formate and glycolate with the rate of formation of hydrogen radical by radiolysis. Additionally, the mole fraction of hydrogen produced by organic radiolysis may be approximated as 1, due to the tendency of formate and glycolate radiolytic products to be soluble in salt solutions, as shown in Figure 2-1. Note that this condition makes the assumption that a negligible amount of CO is formed from the radiolysis of formate and glycolate. Studies aimed at measuring the vapor phase composition of radiolytically-generated gases from organic-bearing solutions have been conducted, and it has been shown that this assumption of CO negligibility is generally valid (primary gaseous decomposition products are H_2, N_2, and O_2).[16] Furthermore, the effect of organic radiolysis on the composition of hydrogen in trapped gas bubbles is, by definition, conservative when the hydrogen mole fraction of the radiolytically-produced gas is 1.

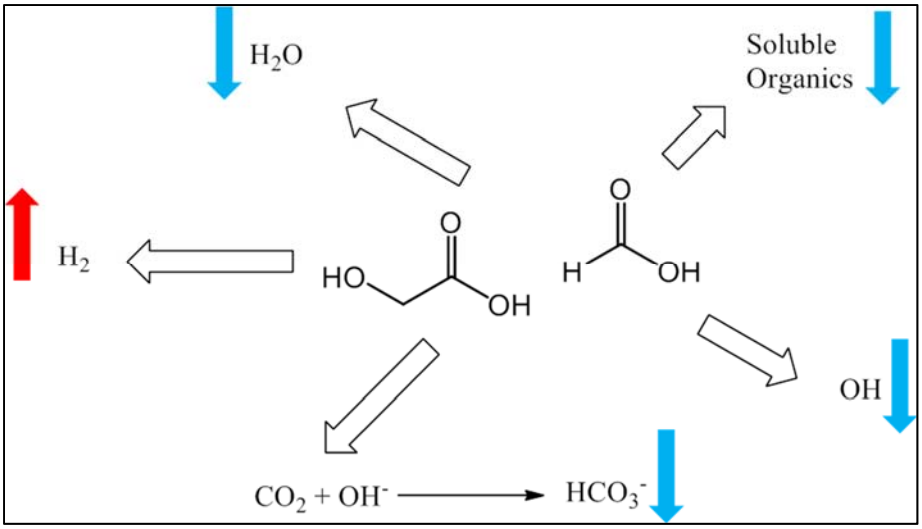

Figure 2-1. Fate of Formate and Glycolate Radiolytic Products. Blue "down" arrows indicate solubility in a caustic aqueous phase, and red "up" arrows indicate offgas production.

The hydrogen calculation method described by Crawford and King combined with the assumption of unity for the hydrogen mole fraction greatly simplify the calculation of organic radiolysis contribution to trapped gas hydrogen composition by defining the total gas production from organic radiolysis as equal to that of hydrogen production from organic radiolysis. Note that the underlying Crawford and King model for formate and glycolate radiolysis has not been validated across all conditions and additional testing is required.

2.4 Effects of Organic Thermolysis on Bubble Compositions

Similarly, Crawford and King[1] described a method to calculate the contribution of formate and glycolate thermolysis on hydrogen production from radioactive wastes. Formate was considered inactive towards thermolytic production of H_2; thermolysis of formate will not be considered in this report. Glycolate thermolysis was approximated by using experimental data for glycolate destruction reported by Ashby.[2] Hydrogen production by glycolate thermolysis is approximated by Equation [15]:

$$HGR_{thermolysis} = \frac{0.0004[NO_2][Al][Glycolate]}{[OH]} e^{\frac{113{,}000}{8.314}\left(\frac{1}{T(^\circ C)+273.15}-\frac{1}{393.15}\right)} \quad [15]$$

where $HGR_{thermolysis}$ is the production rate of hydrogen gas in moles per liter per hour, $[NO_2]$, $[Al]$, $[Glycolate]$, and $[OH]$ are the supernatant molarities of nitrite, aluminum, glycolate, and hydroxide (respectively), and T is the temperature in degrees Celsius. Note that the underlying Crawford and King model for glycolate thermolysis has not been validated across all conditions and additional testing is required.

Similarly, an approximation of the temperature-dependent hydrogen mole fraction of glycolate thermolytic offgas may be made using data reported by Ashby. Using production rates of hydrogen (r_{H_2}) and total gas (r_{TG}) at two temperatures (90 °C and 120 °C) and an assumption of similar reaction mechanisms, the temperature-dependent hydrogen composition may be calculated according to Equations [16] through [19]:

$$r_{H_2} = \frac{C_1 e^{-E_1/RT}\left[Glycolate\right]^{\alpha}\left[NO_2\right]^{\beta}\left[Al\right]^{\gamma}}{\left[OH\right]^{\delta}} \quad [16]$$

$$r_{TG} = \frac{C_2 e^{-E_2/RT}\left[Glycolate\right]^{\alpha}\left[NO_2\right]^{\beta}\left[Al\right]^{\gamma}}{\left[OH\right]^{\delta}} \quad [17]$$

$$\frac{r_{H_2}}{r_{TG}} = y_g^t = \frac{C_1 e^{-E_1/RT}\left[Glycolate\right]^{\alpha}\left[NO_2\right]^{\beta}\left[Al\right]^{\gamma}\left[OH\right]^{\delta}}{C_2 e^{-E_2/RT}\left[Glycolate\right]^{\alpha}\left[NO_2\right]^{\beta}\left[Al\right]^{\gamma}\left[OH\right]^{\delta}} = C' e^{-E'/T} \quad [18]$$

$$\ln\left(y_g^t\right) = \ln\left(C'\right) - \frac{E'}{T} \quad [19]$$

where C_1 and C_2 are the assumed pre-exponential factors for hydrogen production and total gas production (respectively), and E_1 and E_2 are the associated activation energies for hydrogen and total gas production (respectively). Composition data reported by Ashby may be plotted as a linear function of $1/T$ (according to Equation [19]), which allows for the calculation of the modified kinetic parameters C' and E' and subsequent calculation of y_g^t according to Equation [18].

2.5 Oxygen Depletion by Organics

Oxygen depletion by organics occurs through a number of complicated mechanisms including radical combination and direct organic oxidation. When examining glycolate thermolysis in radioactive waste simulants, Ashby noted significant removal of oxygen due to the presence of organic species. Similarly, Bradley has reported the apparent effect of organics to increase the hydrogen composition of trapped gases in radioactive waste streams, and has attributed it to oxygen depletion by organics.[16] Given the complicated reaction kinetics and compound-dependent behavior present in oxygen depletion, it is best to consider a conservatively bounding approach to estimate oxygen consumption rates.

First, an assumption may be made that atmospheric oxygen is not available for depletion. This is generally expected to be true in the case of trapped gases. Peterson has reported that more than 18 inches of sludge are required before an appreciable amount of gas can be trapped and that mixing (or "sloshing") causes a release of gas.[17] These observations are consistent with the assumption that trapped gas is not in contact with the atmosphere and is only exposed gases generated in the waste medium. This assumption is the basis for a first estimation: the rate of oxygen consumption is bounded by the rate of oxygen production by salt solution radiolysis.

Second, an assumption may be made suggesting that organic "fuels" may, in some cases, limit the amount of oxygen that can be absorbed. Oxygen consumption by organics has been reported to be significantly species-dependent.[16] Therefore, knowledge of the tendency for each species to react with oxygen (directly or indirectly) must be applied in order to completely account for consumption of oxygen by organics. In the cases of formate and glycolate, bounding arguments may be established to limit the amount of "fuel" available to consume oxygen.

The use of competition kinetics described by Bibler[15] provides a framework for establishing a maximum theoretical generation rate for reactive organic intermediates derived from the radiolysis of formate and

glycolate. The rate of oxygen consumption must be, by definition, lower than or equal to the rate of formation of these organic intermediates. It follows, then, that a conservative estimation of oxygen consumption by these organic intermediates may be derived by assuming that the rate of oxygen consumption is equal to the rate of formation of these radiolytic products. This rate is equal to the rate of hydrogen formation by radiolysis. Reaction equations showing these steps are shown in Figure 2-2.

$$R\text{-}H + H\cdot \rightarrow H_2 + R\cdot$$
$$R\cdot + O_2 \rightarrow R\text{-}O_2\cdot$$

Figure 2-2. Reaction Equations Describing Secondary Radiolysis of Organics and Subsequent Oxygen Consumption.

A similar argument may be made for the thermolysis of glycolate, given that the reaction rate equation for hydrogen generation reported by Crawford and King is derived from glycolate consumption rates, not hydrogen production rates.

The assumption that the rate of organic intermediate formation (equal to the rate of hydrogen production in the cases of formate and glycolate) can limit the amount of oxygen consumed is the basis for a second estimation: the rate of oxygen consumption is bounded by the rate of hydrogen production from organic species. This assumption is expected to be conservative due to the fact that oxidation by oxygen is only expected for a fraction of organic hydrogen generation products. It is important to note that these assumptions only apply to formate and glycolate. Evaluation of other organic species should be performed before they are integrated into this calculation method.

2.6 Quality Assurance

Requirements for performing reviews of technical reports and the extent of review are established in Manual E7, Procedure 2.60.[18] SRNL documents the extent and type of review using the SRNL Technical Report Design Checklist contained in WSRC-IM-2002-00011, Rev. 2.[19]

3.0 Results and Discussion

3.1 Estimation of Salt Contributions

3.1.1 Effect of Nitrate on Bubble Compositions

Table 3-1 gives literature data for the hydrogen mole fraction of gases produced by radiolysis of nitrate-containing salt solutions (i.e., H_{mix}).

Table 3-1. Literature Data for Hydrogen Mole Fraction of Gas Produced from Nitrate Solution Radiolysis.

Nitrate Concentration (M)	Hydrogen Fraction, H_{mix}	Reference
0.0001	0.710	Bradley, 1971[16]
0.001	0.670	Bradley, 1971[16]
0.01	0.690	Bradley, 1971[16]
0.1	0.700	Bradley, 1971[16]
0.5	0.560	Bradley, 1971[16]
1	0.314	Mahlman, 1961[20]
2	0.123	Peterson, 1998[21]
2	0.160	Mahlman, 1961[20]
3	0.097	Mahlman, 1961[20]
4	0.071	Mahlman, 1961[20]
4	0.180	Bradley, 1971[16]
5	0.059	Mahlman, 1961[20]
6	0.044	Mahlman, 1961[20]
7	0.034	Mahlman, 1961[20]

A subset of the data shown in Table 3-1 was used by Hester[12] to develop a mathematical model for the prediction of radiolytic gas hydrogen composition as a function of nitrate concentration. That model is recreated in Figure 3-1 below.

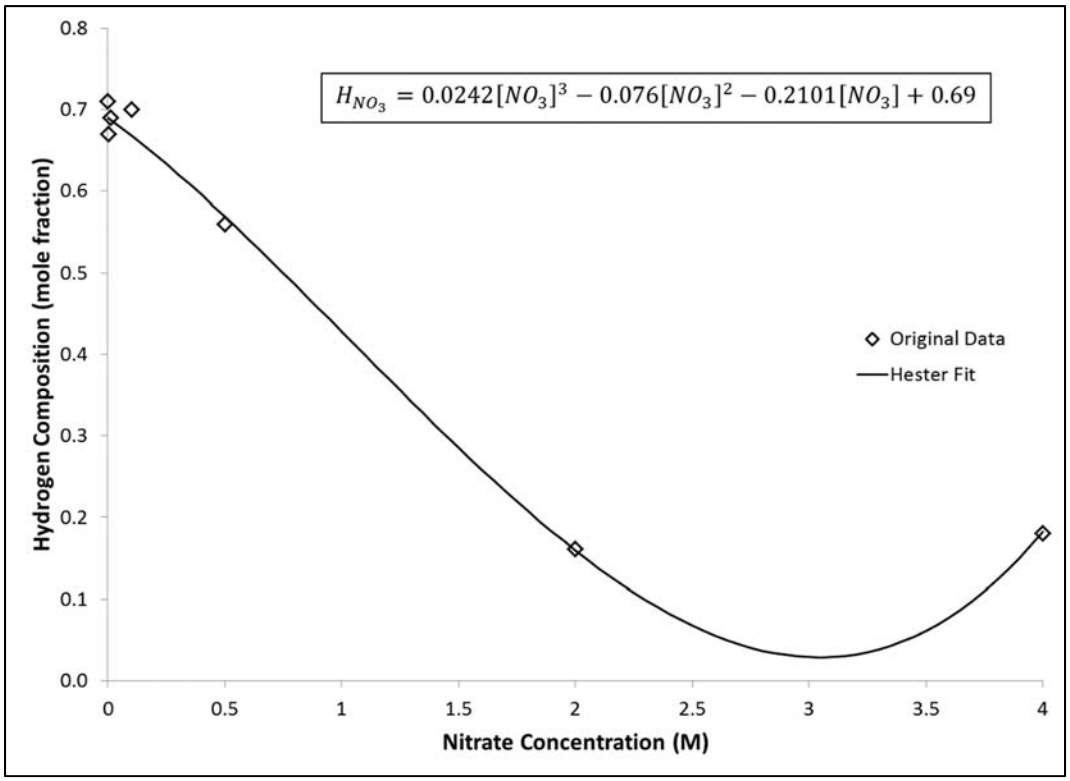

Figure 3-1. Data Employed by Hester for Nitrate Effect on Hydrogen Composition in Radiolytic Offgas. The black line represents the model derived from the data.

The nitrate model employed by Hester suffers from a few drawbacks. First, and most importantly, the model is unconservative for hydrogen composition at nitrate concentrations between 2 and 4 M. Hester's

nitrate model predicts that a 3 M nitrate solution will produce a gas composed of 3% H_2 upon radiolysis, whereas data from Mahlman suggests that such a solution will actually yield a hydrogen composition closer to 10%. Second, Hester's nitrate model predicts a large increase in hydrogen composition at nitrate concentrations greater than 4 M, and is incapable of yielding a physically meaningful value for solutions of nitrate concentration higher than 5.2 M. Contrary to the model-predicted behavior, data from Mahlman suggests that hydrogen composition of radiolytically-formed gases decreases continuously as a function of nitrate concentration, with a gas composition of 3.4% H_2 yielded from radiolysis of a 7 M nitrate solution.

Figure 3-2 is a graphical representation of the data given in Table 3-1.

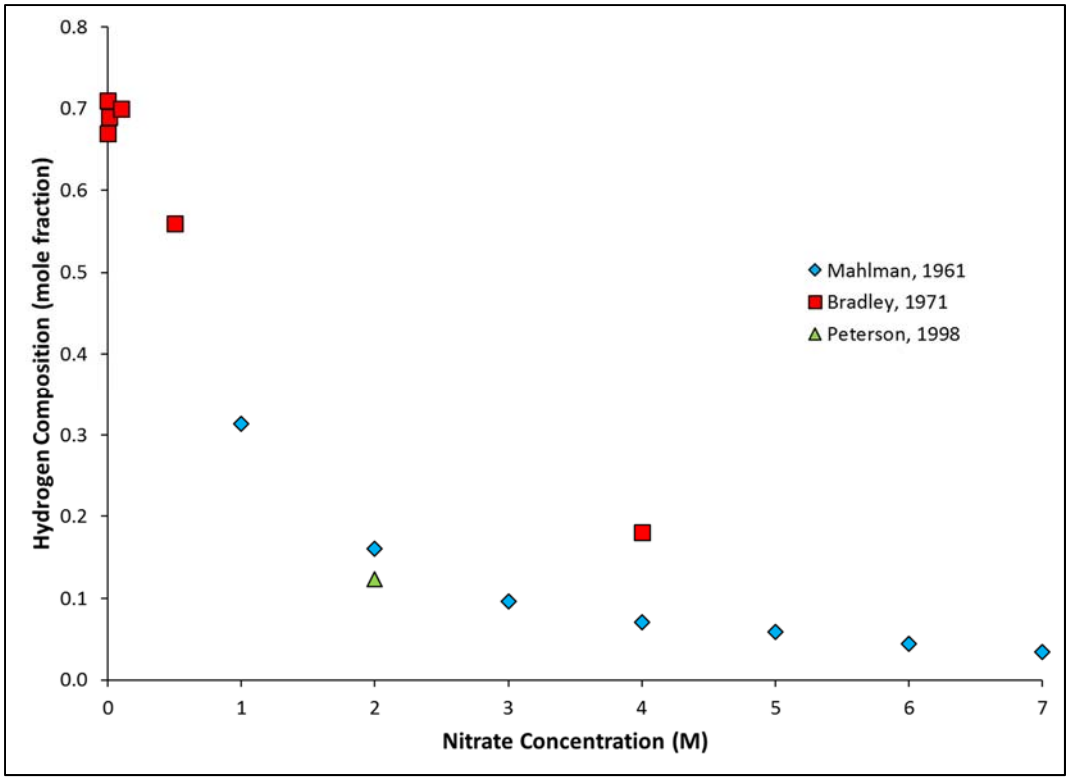

Figure 3-2. Plot of Available Data Describing the Effect of Nitrate on Hydrogen Composition.

Upon inspection of the data shown in Figure 3-2, it is clear that hydrogen composition of radiolytically-generated gas tends to diminish with increasing nitrate concentration. This behavior may be expressed mathematically as an exponential or inverse relationship, leading to a number of possible alternative fits to the literature data. Additional fits may be derived by varying importance on "goodness of fit" relative to bounding behavior and conservatism.

By fitting an exponential curve to all of the data presented in Figure 3-2, a relatively simple model for hydrogen composition as a function of nitrate concentration may be derived, yielding the relationship described in Equation [20] below:

$$y_w^r = 0.5703e^{-0.442[NO_3]} \quad [20]$$

While this model correctly predicts hydrogen composition behavior at high nitrate concentrations, it is significantly under predictive of hydrogen composition at lower nitrate concentrations. In order to generate a conservative exponential model, one may simply use the data reported by Bradley for hydrogen composition at 0.1 and 4 M nitrate (hydrogen fractions of 0.7 and 0.18, respectively) and generate a similar function using this limited subset of data. The results of such an analysis are shown in Equation [21] below:

$$y_w^r = 0.7241e^{-0.348[NO_3]} \quad [21]$$

The contours of the best fit and conservative exponential equation models are shown in Figure 3-3, along with the literature data previously discussed. The Hester fit is shown for convenient comparison.

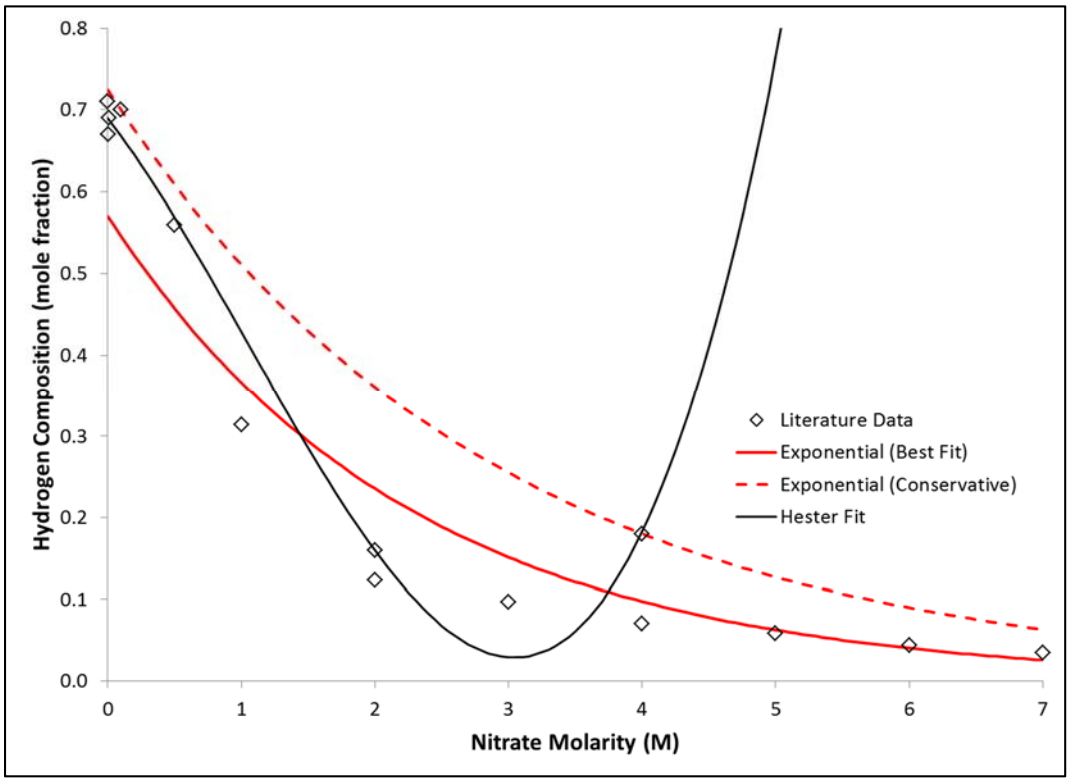

Figure 3-3. Plot of Two Suggested Exponential Models for Nitrate Effect on Hydrogen Composition.

A number of observations can be made upon inspection of the exponential models shown in Figure 3-3. First, as mentioned earlier, it is obvious that the "best-fit" exponential model significantly under predicts hydrogen composition at nitrate concentrations lower than 0.5 M. This problem is avoided in the "conservative" exponential model; however, the conservative model tends to significantly overpredict hydrogen composition at moderate nitrate concentrations (between 0.5 and 4 M). Both exponential models are superior to Hester's nitrate model in describing high nitrate (>4 M) concentration behavior.

Alternatively, a piecewise inverse-linear model may be used to describe the relationship between hydrogen composition and nitrate concentration. By using the 1 M nitrate data point reported by Mahlman as a joint, one may fit a linear curve to hydrogen composition data at concentrations lower than 1 M while fitting an inverse linear curve to hydrogen composition data at concentrations higher than 1 M. This exercise returns

a separate hydrogen composition model, shown below in Equations [22] and [23], referred to as the "best fit" inverse model.

$$y_w^r([NO_3] < 1M) = -0.3948[NO_3] + 0.7069 \quad [22]$$

$$y_w^r([NO_3] \geq 1M) = \frac{0.3067}{[NO_3]} + 0.0073 \quad [23]$$

The best-fit inverse model describes well the reported hydrogen compositions as a function of nitrate concentration with the exception of the 4 M nitrate data point reported by Bradley (hydrogen fraction of 0.18). While this data point is suspect due to the presence of lower hydrogen compositions reported by Mahlman and Peterson at lower nitrate concentrations, it may be of use to correct the inverse model described above in order to bound this data point. This correction may be performed by using the 0.5 M data point reported by Bradley as the point of discontinuity (rather than the 1 M data point) and the 0.1 M and 4 M points reported by Bradley to fit the linear and inverse linear curves, respectively. The results of this exercise are shown in Equations [24] and [25], which comprise the "conservative" inverse model.

$$y_w^r([NO_3] < 0.5M) = -0.35[NO_3] + 0.735 \quad [24]$$

$$y_w^r([NO_3] \geq 0.5M) = \frac{0.2171}{[NO_3]} + 0.1257 \quad [25]$$

The contours of the best fit and conservative inverse equation models are shown in Figure 3-4, along with the literature data previously discussed. The Hester fit is shown for convenient comparison.

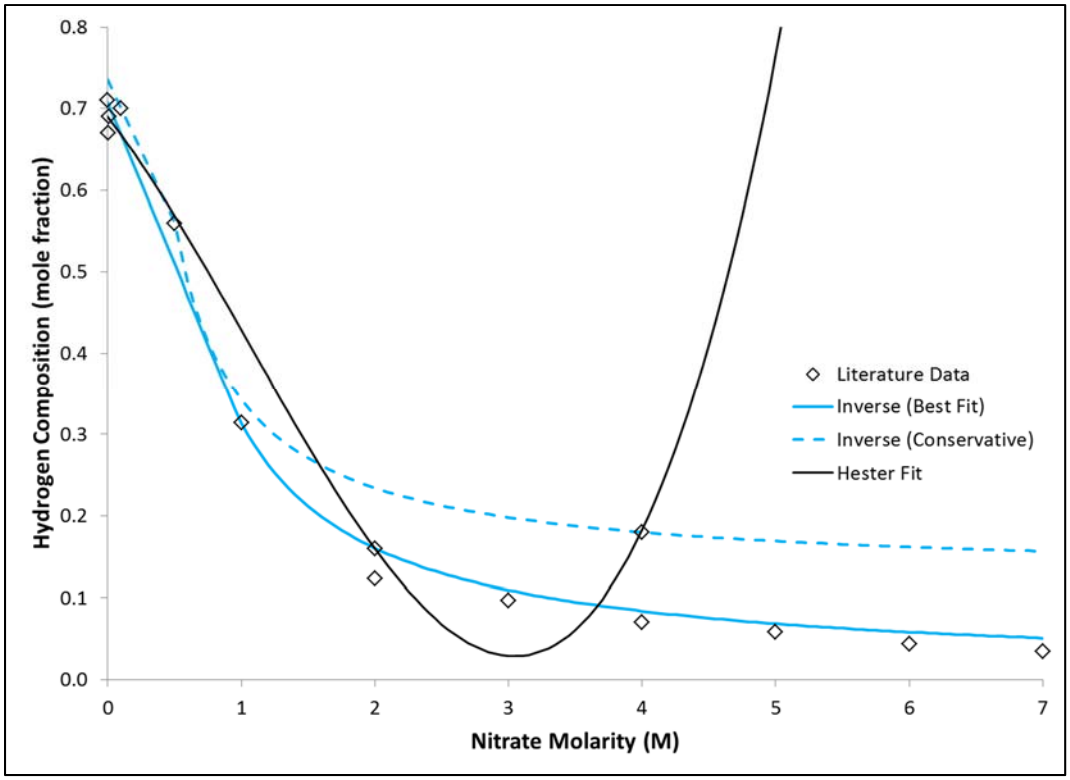

Figure 3-4. Plot of Two Suggested Inverse Linear Models for Nitrate Effect on Hydrogen Composition.

The trends shown in Figure 3-4 show the superior ability of the piecewise inverse equation models to describe hydrogen composition behavior as a function of nitrate concentration. It is important to note that the conservative inverse model significantly overpredicts the hydrogen composition of gases produced from solutions of 4 M nitrate or greater. This is due to the exclusion of data other than the 4 M nitrate point reported by Bradley (hydrogen composition of 0.18).

Table 3-2 lists the literature data (seen previously in Table 3-1) as well as the calculated hydrogen composition according to each of the five models (Hester, best-fit exponential (BF-EXP), conservative exponential (C-EXP), best-fit inverse (BF-INV), and conservative inverse (C-INV)) and the corresponding sum of square residuals for each model.

Table 3-2. Evaluation of Fit Quality for Nitrate Radiolytic Effect Models.

Reference	Nitrate (M)	H_2 Mole Fraction, H_{mix} (measured)†	Hester	BF-EXP	C-EXP	BF-INV	C-INV
Bradley, 1971	0.0001	0.710	0.690	0.570	0.724	0.707	0.735
Bradley, 1971	0.001	0.670	0.690	0.570	0.724	0.707	0.735
Bradley, 1971	0.01	0.690	0.688	0.568	0.722	0.703	0.732
Bradley, 1971	0.1	0.700	0.668	0.546	0.699	0.667	0.700
Bradley, 1971	0.5	0.560	0.569	0.457	0.608	0.510	0.560
Mahlman, 1961	1	0.314	0.428	0.367	0.511	0.314	0.343
Peterson, 1998	2	0.123	0.159	0.236	0.361	0.161	0.234
Mahlman, 1961	2	0.160	0.159	0.236	0.361	0.161	0.234
Mahlman, 1961	3	0.097	0.029	0.151	0.255	0.110	0.198
Mahlman, 1961	4	0.071	0.182	0.097	0.180	0.084	0.180
Bradley, 1971	4	0.180	0.182	0.097	0.180	0.084	0.180
Mahlman, 1961	5	0.059	0.765	0.063	0.127	0.069	0.169
Mahlman, 1961	6	0.044	1.921	0.040	0.090	0.058	0.162
Mahlman, 1961	7	0.034	3.796	0.026	0.063	0.051	0.157
		R^2	**0.042**	**0.943**	**0.920**	**0.984**	**0.983**

†Measured H_{mix} values are calculated from raw measurements of H2 and O2 formation from radiolytic experiments.

The most representative fits to the available hydrogen composition-nitrate concentration data appear to be the inverse function models, with the "best-fit" inverse model returning an R^2 value of 0.984 and the "conservative" inverse model yielding an R^2 value of 0.983. Exponential models perform reasonably well, with the "best fit" exponential model yielding an R^2 value of 0.943 relative to the R^2 value of 0.920 achieved by the "conservative" exponential model. The least applicable model is the Hester fit, yielding an R^2 value of 0.042. Given these results and the stipulations concerning the single point at 4 M reported by Bradley, it is recommended that nitrate contributions to hydrogen composition from radiolysis of nitrate-containing solutions utilize the "best-fit" inverse model, described in Equations [22] and [23]. For the remainder of this report, this model will be used when estimations of nitrate effect on hydrogen composition are needed.

3.1.2 Effect of Nitrite on Bubble Compositions

Table 3-3 gives literature data for the hydrogen composition of gases produced by radiolysis of nitrite-containing salt solutions.[16]

Table 3-3. Literature Data for Hydrogen Composition of Gas Produced from Nitrite Solution Radiolysis.

Nitrite Concentration (M)	Hydrogen Mole Fraction, H_{mix}
0.01	0.97
0.1	0.87
0.5	0.09
1	0.78
2	0.80
3	0.85

This data was employed by Hester to generate a mathematical model for the prediction of radiolytic gas hydrogen composition as a function of nitrite composition. That model is recreated in Figure 3-5 below.

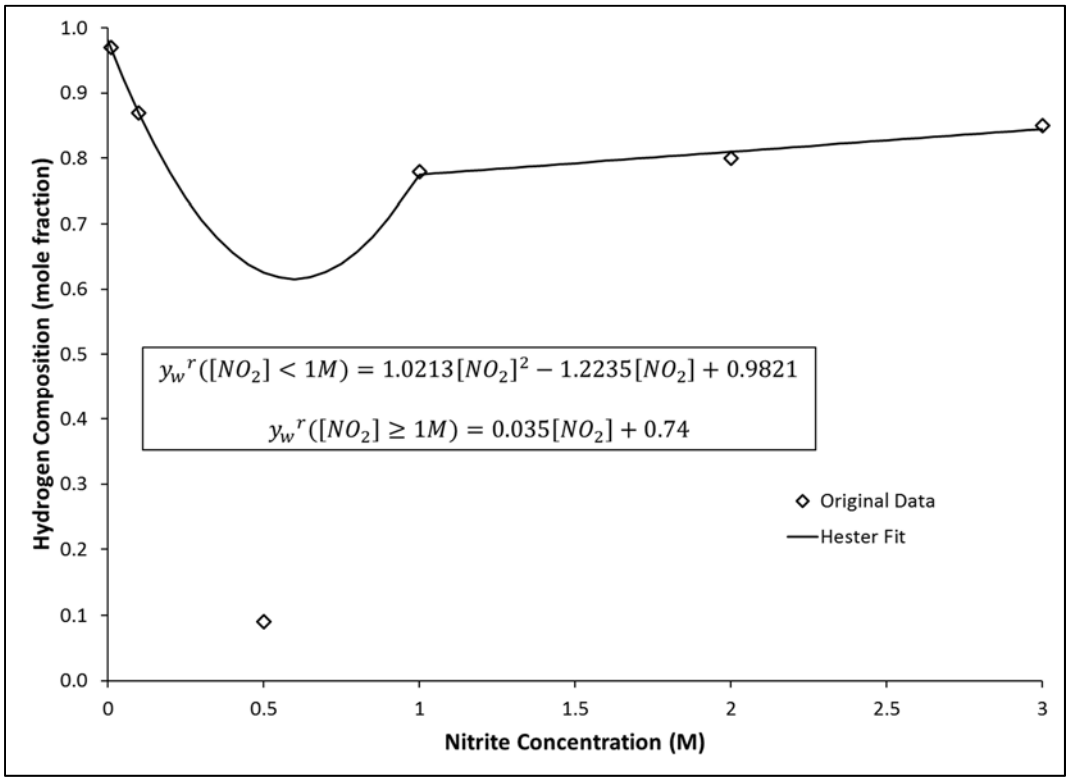

Figure 3-5. Data Employed by Hester for Nitrite Effect on Hydrogen Composition in Radiolytic Offgas. The black line represents the model derived from the data.

Upon inspection of the trend presented in Figure 3-5, a couple of challenges are evident concerning the applicability of the Hester nitrite model. First, the model predicts a significant decrease in hydrogen composition at nitrite concentrations around 0.5 M. This is due to the attempt to include a hydrogen composition of 0.09 reported by Bradley from a 0.5 M nitrite solution. However, literature reports suggest that nitrite does not play a strong role in the hydrogen composition of radiolytic gas, and the fact that the 0.5 M data point is so significantly removed from the other data suggests that this may be an erroneous data point, and should be left out of curve fitting. As a result, this region of the Hester nitrite model (0.1 M to 1 M) may be under predictive of hydrogen composition. Second, the nitrite model predicts that hydrogen composition increases with increasing nitrite concentration at high nitrite loadings (>1 M). This is counterintuitive, given that nitrite is expected to slow the production of hydrogen gas.

An improved model to describe hydrogen composition as a function of nitrite loading may be an exponential function with a large slope at low nitrite concentrations (to account for the decrease in hydrogen composition from 0.97 to 0.78 between 0.01 and 1 M nitrite) and a large intercept (to account for the relatively constant behavior of hydrogen compositions at nitrite concentrations above 1 M). Such a model is given in Equation [26] below.

$$y_w^r = 0.15e^{-8.0265[NO_2]} + 0.85 \quad [26]$$

In this exponential nitrite model, a constant of 0.85 is employed in order to bound the highest measured hydrogen composition in the high-nitrite (>1 M) regime. A pre-exponential factor of 0.15 is used in order to set the hydrogen composition from pure water radiolysis to a value of 1 (thereby bounding the value of

0.97 at 0.01 M nitrite). A value of -8.0265 was found to be the numerical solution to the transcendental equation developed by setting the derivative of hydrogen composition with respect to nitrite concentration equal to the approximate numerical derivative at 0.01 M (calculated using data from 0.01 M and 0.1 M).

A contour of this suggested model is given in Figure 3-6, along with literature data and the Hester model for comparison.

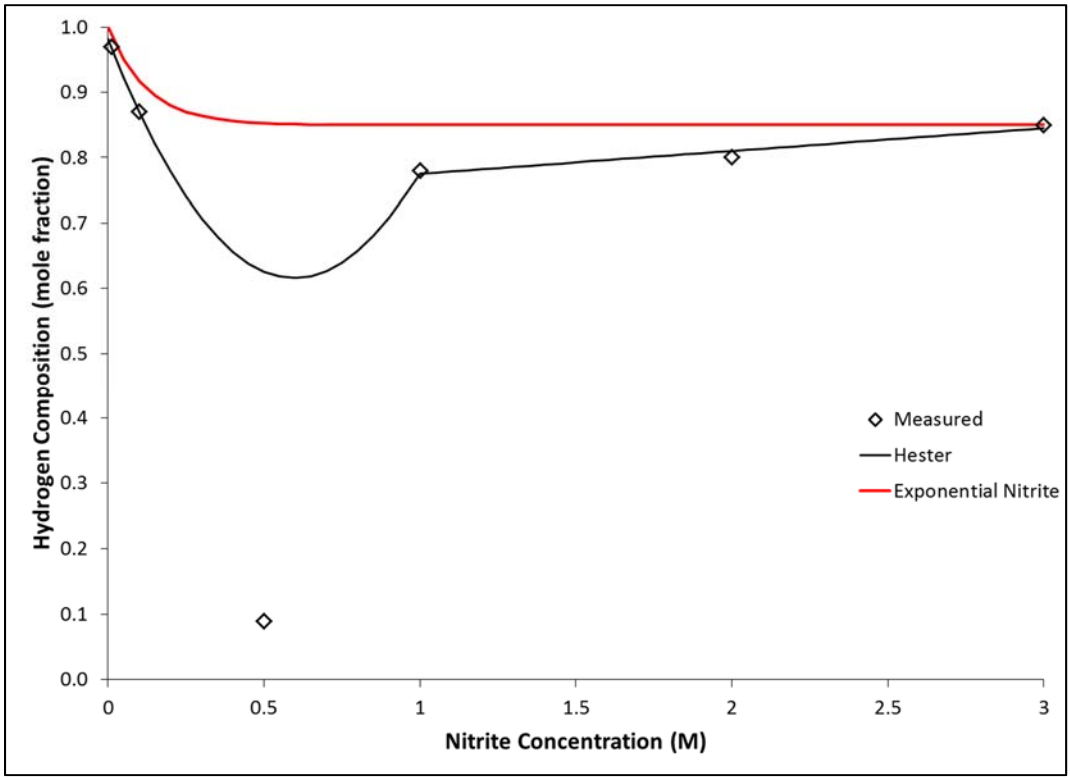

Figure 3-6. Plot of Suggested Exponential Model for Nitrite Effect on Hydrogen Composition.

Strictly speaking, the exponential nitrite model is only a slight improvement over the existing Hester nitrite model in terms of conservatism and applicability. The fact that the exponential model predicts a higher hydrogen composition at 0.5 M along with the fact that it does not predict an increase of hydrogen composition with increasing nitrite suggests that the exponential nitrite model is more valid than the Hester nitrite model. However, due to the nature of the curve fits employed, the Hester curve remains the more accurate of the two models with an R^2 value of 0.99 relative to the R^2 value of 0.87 achieved by the exponential nitrite model. It is important to note here that these metrics are dependent on the reliability of the limited amount of data available. Additional data from radiolysis of nitrite solutions may justify the need to reevaluate the validity of these two models. For the purposes of this report, the exponential nitrite model is recommended for use due to its relative simplicity and reduced probability of underprediction of hydrogen composition at low nitrite concentrations.

3.1.3 Calculation of Bubble Compositions in Salt Blends

Table 3-4 gives literature data for the hydrogen composition of gases produced by radiolysis of solutions containing nitrate and nitrite.

Table 3-4. Literature Data for Hydrogen Composition of Gas Produced from Mixed Nitrate and Nitrite Solution Radiolysis.

Nitrite Concentration (M)	Nitrate Concentration (M)	Hydrogen Mole Fraction, H_{mix}	Reference
0.5	2	0.174	Peterson[21]
1	2	0.187	Peterson[21]
1	2	0.123	Peterson[21]
1	2	0.160	Peterson[21]
1.3	2.7	0.082	DPST-72-122-2[22]
1.6	2	0.200	Peterson[21]
2	4	0.180	Bradley[16]

By using the models developed in Sections 3.1.1 and 3.1.2 in conjunction with the mathematical method described in Section 2.2, one may calculate the expected hydrogen composition from radiolysis of a solution containing both nitrite and nitrate. In order to perform this calculation, one must modify Equations [4], [5], and [6] such that the variables H_{NO_3} and H_{NO_2} are redefined in terms of the Best-Fit Inverse and Exponential Nitrite models, respectively. These corrections are shown in Equations [27], [28], and [29] below.

$$H_{NO_3}([NO_3] < 1M) = -0.3948[NO_3] + 0.7069 \quad [27]$$

$$H_{NO_3}([NO_3] \geq 1M) = \frac{0.3067}{[NO_3]} + 0.0073 \quad [28]$$

$$H_{NO_2} = 0.15e^{-8.0265[NO_2]} + 0.85 \quad [29]$$

Table 3-5 lists the reported hydrogen composition from the experiments listed in Table 3-4 as well as the predicted hydrogen composition using the calculation described above.

Table 3-5. Evaluation of Mixed Nitrate/Nitrite Model with Verification Data.

Nitrite (M)	Nitrate (M)	Hydrogen Mole Fraction, H_{mix} (Measured)	Hydrogen Mole Fraction, H_{mix} (Calculated)	Difference (mole % H_2)
0.5	2	0.174	0.157	-1.7
1	2	0.187	0.171	-1.6
1	2	0.123	0.171	4.8
1	2	0.160	0.171	1.1
1.3	2.7	0.082	0.140	5.8
1.6	2	0.200	0.195	-0.5
2	4	0.180	0.141	-3.9

The data in Table 3-5 suggests that the calculation method described above predicts hydrogen composition of the gases produced by radiolysis of nitrite- and nitrate-containing solutions reasonably well, within less than 6 mole percent in the most over-conservative case and within less than 4 mole percent in the most under-conservative case. It is recommended that this model be used to calculate the effects of nitrite/nitrate solution radiolysis on trapped gas bubble hydrogen composition prediction going forward.

3.2 Estimation of Organic Contributions

3.2.1 Effect of Formate and Glycolate Radiolysis on Bubble Compositions

A method for calculating the hydrogen generation rate due to formate and glycolate radiolysis has been previously proposed by Crawford and King.[1] Using this method and the assumptions stated in Section **Error! Reference source not found.**, one may predict the contribution of formate and glycolate radiolysis using the hydrogen radical reactivities shown in Table 3-6.

Table 3-6. Rate Constants for Hydrogen Radical Reactions.[1]

Species	Rate Constant for Reaction with H Radical
Nitrate	1.4×10^6
Nitrite	7.1×10^8
Hydroxide	2.2×10^7
Formate	2.1×10^8
Glycolate	4.6×10^7

The estimation of contribution is performed by assuming that all non-hydrogen products from organic radiolysis are retained in the aqueous phase upon formation, thereby fixing the hydrogen composition of the radiolytic offgas from organics at 100%.

3.2.2 Effect of Formate and Glycolate Thermolysis on Bubble Compositions

It has been shown that formate exhibits little to no thermolytic behavior toward the production of hydrogen gas in caustic conditions.[1] Therefore, only glycolate is considered here. Ashby reported the thermolytic degradation of glycolate to produce hydrogen, nitrogen, and nitrous oxide gases.[2] The reaction dynamics were explored and summarized by Crawford and King, and are not replicated here. It was shown that Equation [15] may be used to approximate the rate of hydrogen formation due to glycolate thermolysis as a function of temperature. Given this expression, it is only necessary to know the dependence of thermolytic offgas composition as a function of temperature in order to estimate the effect of glycolate thermolysis on trapped gas bubble hydrogen composition.

Ashby reported the amounts of hydrogen, nitrogen, and nitrous oxide produced by glycolate thermolysis at 90 °C and at 120 °C.[2] Figure 3-7 displays the data reported for glycolate degradation at 90 °C, and Figure 3-8 displays the data reported at 120 °C. In both figures, curves have been fit to the linear regime of the reaction in order to determine relative rates of formation for total gas and hydrogen.

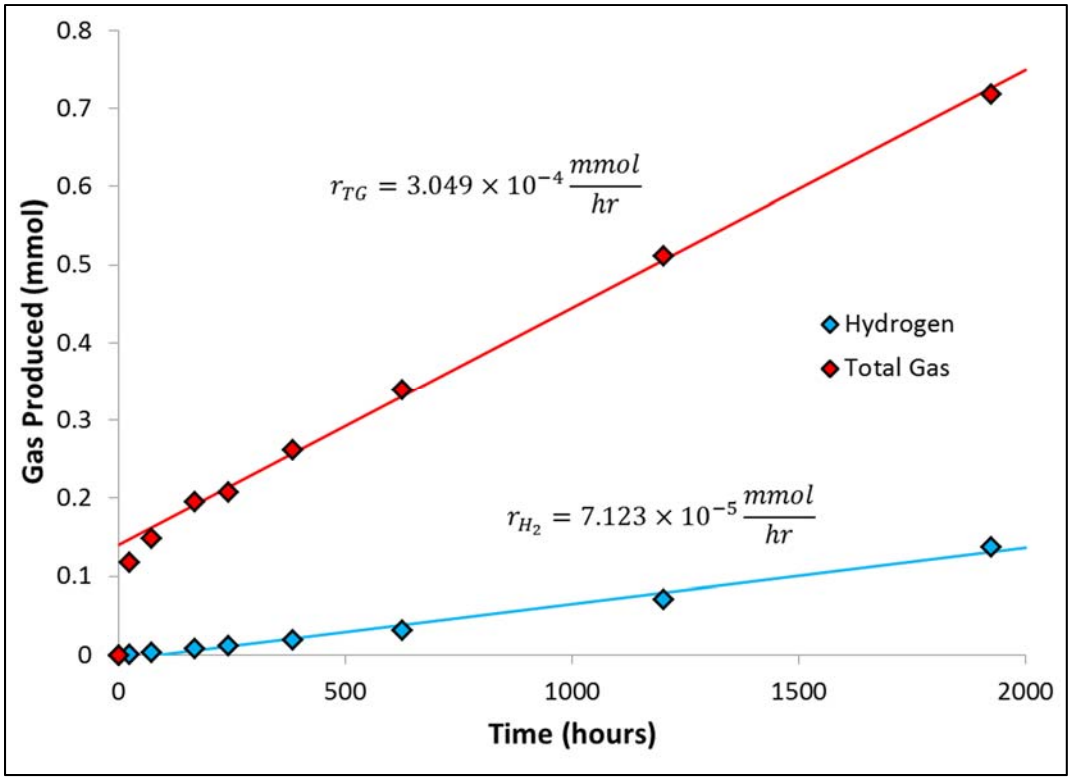

Figure 3-7. Gas Generation from Glycolate Thermolysis at 90 °C Under Ar Atmosphere.

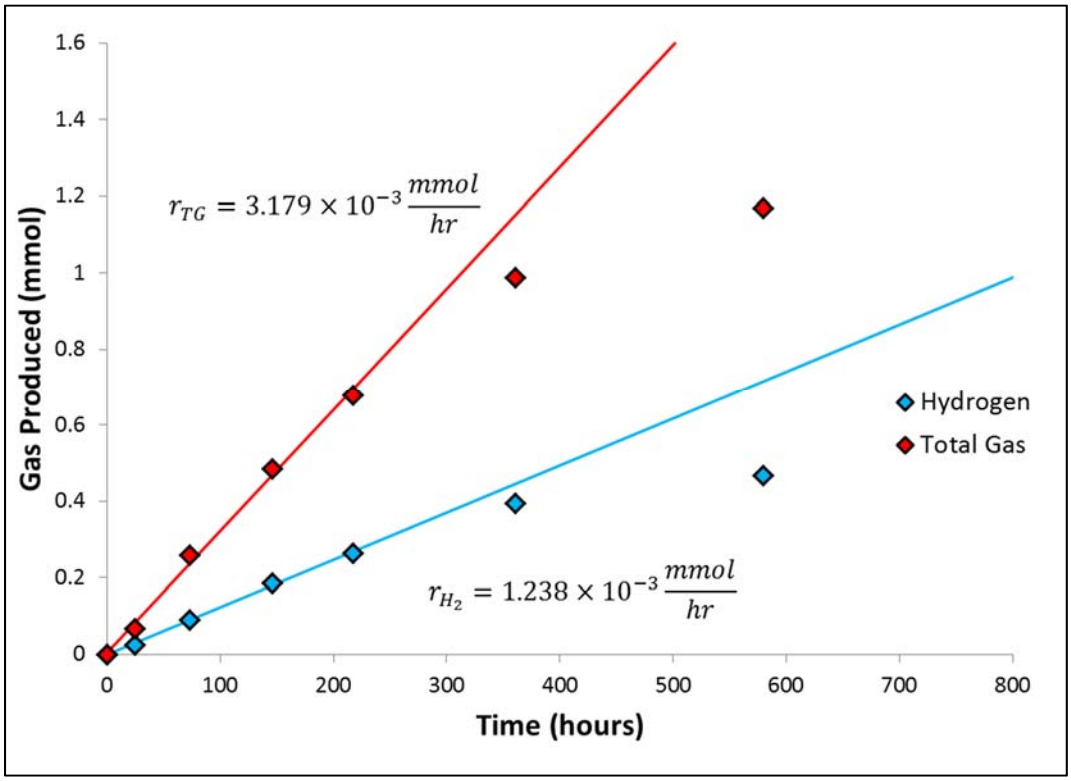

Figure 3-8. Gas Generation from Glycolate Thermolysis at 120 °C Under Ar Atmosphere.

It is important to note that the ratio of hydrogen generation rate and total gas production rate is equal to the hydrogen mole fraction of thermolytic offgas at the specified temperature, as is shown in Equation [30].

$$\frac{r_{H_2}(T)}{r_{TG}(T)} = y_g^t(T) \qquad [30]$$

Using the relationships described in Equations [19] and [30] as well as the data shown in Figure 3-7 and Figure 3-8, one may easily solve for the pre-exponential factor C' and modified activation energy E' required to calculate the thermolytic offgas hydrogen composition with the use of a semilog plot, as shown in Figure 3-9.

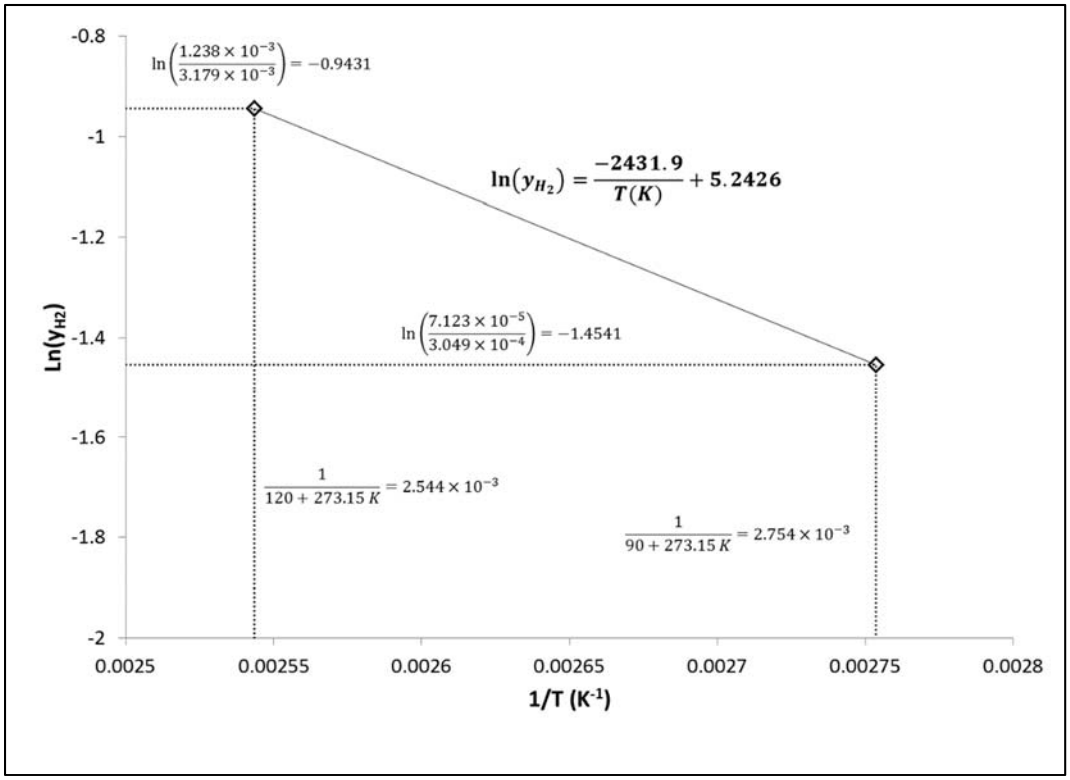

Figure 3-9. Arrhenius Plot of Glycolate Thermolytic Rate Data.

By solving for the pre-exponential factor $C' = e^{5.2426} = 189.161$ and modified activation energy $E' = -(-2431.9) = 2431.9$ (shown in Figure 3-9), one arrives at the following expression for thermolytic hydrogen composition as a function of temperature (Equation [31]):

$$y_g^t(T) = 189.161 e^{\frac{-2431.9}{T(^\circ C)+273.15}} \qquad [31]$$

The contour of y_g^t as a function of T is given in Figure 3-10.

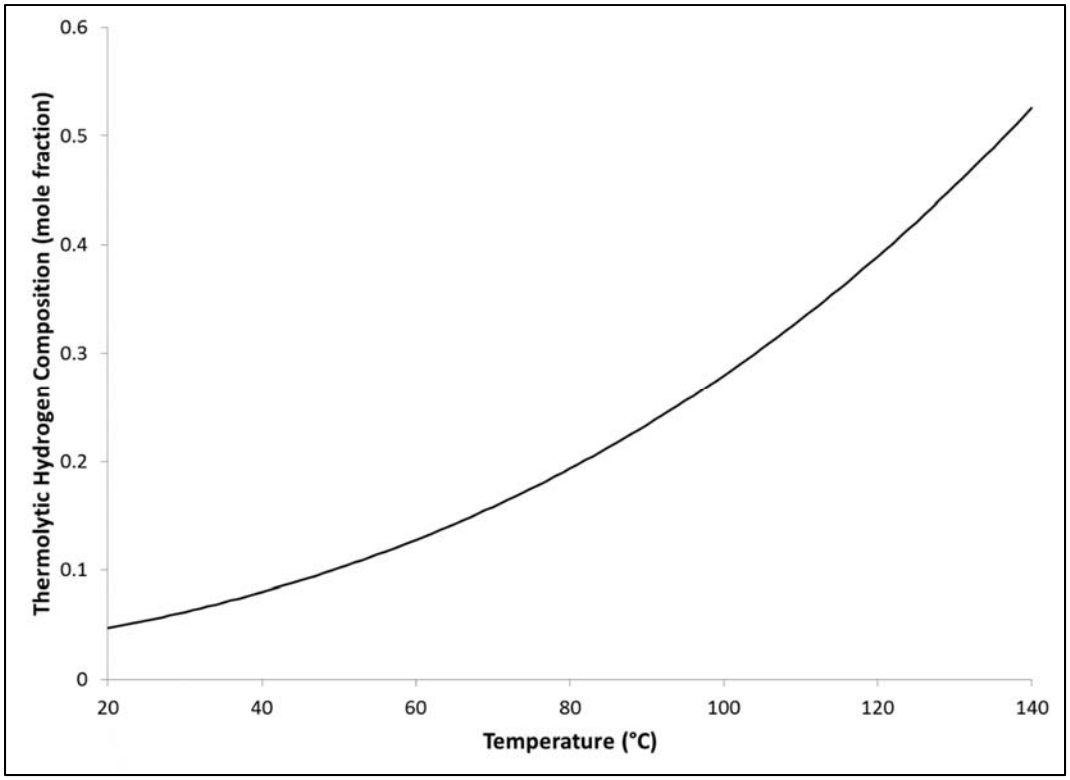

Figure 3-10. Predicted Glycolate Thermolytic Hydrogen Composition as a Function of Temperature.

As is obvious from Equation [31] and Figure 3-10, the calculated response of hydrogen composition to increasing temperature is non-linear, suggesting that more than one reaction is responsible for gas production during glycolate thermolysis. It is recommended that these mechanisms be further investigated in order to better understand the thermolytic behavior and products of glycolate in caustic environments.

3.2.3 Estimation of Oxygen Depletion

As mentioned in Section 2.5, oxygen depletion may be estimated by calculating two reaction rates: the rate of hydrogen production by radiolysis and thermolysis involving organics and the rate of oxygen production by solution radiolysis. The least of the two calculated rates is then used as a bounding value for oxygen depletion rate. This may be written as the following expression (Equation [32]), where the hydrogen production terms from radiolysis and thermolysis involving organics is on the left side and oxygen production by solution radiolysis is on the right side:

$$\dot{n}_{OD} = \min\ (y_g^r \dot{n}_g^r + y_f^r \dot{n}_f^r + y_g^t \dot{n}_g^t, \left(1 - y_w^r\right) \dot{n}_w^r) \qquad [32]$$

As described earlier, the hydrogen composition of organic radiolytic gas products may be considered approximately equal to 100%. Additionally, the hydrogen composition of water/salt solution radiolysis gas products may be calculated using the salt solution radiolytic model described in Section 3.1.

3.2.4 Treatment of Organics Other Than Formate and Glycolate

SRS liquid waste is known to contain organics other than formate.[23] These organics are expected to have an impact on the hydrogen composition of trapped gas bubbles by way of radiolysis, thermolysis, and oxygen consumption. Radiolysis of solutions containing TBP and dodecane has been reported by Bradley

and has shown significant effects on hydrogen composition (increasing hydrogen composition from 18 mol% to 90 mol% in the presence of salt solution simulants).[16] Similar behavior was reported by Peterson and Crawford concerning H_2/O_2 ratios of greater than 0.5 in the presence of butanol and dibutylphosphate.[21] Ashby reported the thermolysis of HEDTA in salt solution simulants, leading to the formation of hydrogen, nitrogen, and nitrous oxide gases.[2] These results suggest that organics other than formate have effects on bubble hydrogen composition that are potentially unbounded by the mechanisms described in this report. Investigation of the effects of suspected major organic substituents (other than formate and glycolate) in SRS liquid waste on the hydrogen composition of trapped gas bubbles is beyond the scope of this report, and is recommended in future testing for incorporation into an improved hydrogen composition model.

3.3 Example Calculation

The following is an example calculation designed to illustrate the use of the calculation methods described in the sections above. For the purposes of this example, consider a 1,000,000 L solution (~ 264,200 gallons) of 4 M $NaNO_3$, 2 M $NaNO_2$, 1 M NaOH, 0.5 M $NaAlO_2$ 3,000 mg/L formate, and 10,000 mg/L of glycolate exposed to 30,000 BTU/hr of gamma radiation at 70 degrees Celsius. It should be noted that the nitrate and nitrite concentrations used in this example calculation are the same values used in an example calculation presented by Hester. Concentrations of hydroxide and aluminum are given as examples in order to calculate radiolytic and thermolytic hydrogen generation rates from formate and glycolate thermolysis.

3.3.1 Salt Solution Radiolysis

First, the effects of salt solution radiolysis on the hydrogen composition must be calculated. Using Equations [33] through [40], one may calculate the value for y_w^r in the following manner:

$$H_{NO_3} = \frac{0.3067}{4} + 0.0073 = 0.084 \quad [33]$$

$$H_{NO_2} = 0.15e^{-8.0265(2)} + 0.85 = 0.85 \quad [34]$$

$$F_{NO_3} = \frac{4}{4+2} = 0.667 \quad [35]$$

$$F_{NO_2} = \frac{2}{4+2} = 0.333 \quad [36]$$

$$\left[NO_{eff}\right] = 4 + \tfrac{1}{2}2 = 5M \quad [37]$$

$$C_{NO_3} = \frac{0.466 - 0.51\times 5^{1/3} + 0.14\times 5^{2/3} + 0.0055\times 5}{0.466 - 0.51\times 4^{1/3} + 0.14\times 4^{2/3} + 0.0055\times 4} = 0.986 \quad [38]$$

$$C_{NO_2} = \frac{0.466 - 0.51\times 5^{1/3} + 0.14\times 5^{2/3} + 0.0055\times 5}{0.466 - 0.51\times 1^{1/3} + 0.14\times 1^{2/3} + 0.0055\times 1} = 0.303 \quad [39]$$

$$y_w^r = (0.084)(0.667)(0.986) + (0.85)(0.333)(0.303) = 0.141 \quad [40]$$

It should be noted that the H_{mix} value of 0.141 determined above using the revised H_2 correlations for nitrate and nitrite in this work is ~25% lower than the value of 0.20 derived in Hester for the same nitrate and nitrite concentrations. Once y_w^r has been calculated, $\dot{n}_w^r$ may be found by first calculating the production rate of hydrogen by salt solution radiolysis, $\dot{n}_{H_2}^w$, as described by Boley[14] and shown in Equations [41] and [42] below.

$$G_{H_2}^w = 0.466 - 0.51 \times 5^{1/3} + 0.14 \times 5^{2/3} + 0.0055 \times 5 = 0.031 \frac{molecules\ H_2}{100\ eV} \quad [41]$$

$$\dot{n}_{H_2}^w = 0.031 \frac{molecules\ H_2}{100\ eV} \cdot 30{,}000 \frac{BTU}{hr} \cdot \frac{6.585 \times 10^{21} eV}{BTU} \cdot \frac{1\ mol}{6.022 \times 10^{23} molecules} \quad [42]$$

$$= \frac{0.107\ mol\ H_2}{hr}$$

The production rate of gas by salt solution radiolysis, $\dot{n}_w^r$, is then found by taking the ratio of $\dot{n}_{H_2}^w$ and y_w^r, as shown in Equation [43].

$$\dot{n}_w^r = \frac{\dot{n}_{H_2}^w}{y_w^r} = \frac{0.107}{0.141} = 0.759 \frac{mol}{hr} \quad [43]$$

3.3.2 Formate and Glycolate Radiolysis

Next, one must calculate the effects due to formate and glycolate radiolysis. This may be done by using the reaction rate constants given in Table 3-6 and following the method recommended by Crawford and King,[1] and is shown in Equations [44]-[47].

$$G_{H_2}^f = \frac{0.58\left[HCOO^-\right] r_f}{\sum [i] r_i} = \frac{0.58 \cdot 0.067 \cdot 2.1 \times 10^8}{(0.067 \cdot 2.1 \times 10^8) + (0.133 \cdot 4.6 \times 10^7) + (4 \cdot 1.4 \times 10^6) + (2 \cdot 7.1 \times 10^8) + (1 \cdot 2.2 \times 10^7)} \quad [44]$$

$$= 0.0056 \frac{molecules\ H_2}{100\ eV}$$

$$G_{H_2}^g = \frac{0.58\left[C_2H_3O_3^-\right] r_g}{\sum [i] r_i} = \frac{0.58 \cdot 0.133 \cdot 4.6 \times 10^7}{(0.067 \cdot 2.1 \times 10^8) + (0.133 \cdot 4.6 \times 10^7) + (4 \cdot 1.4 \times 10^6) + (2 \cdot 7.1 \times 10^8) + (1 \cdot 2.2 \times 10^7)} \quad [45]$$

$$= 0.0024 \frac{molecules\ H_2}{100\ eV}$$

$$\dot{n}_f^r = 0.0056 \frac{molecules\ H_2}{100\ eV} \cdot 30{,}000 \frac{BTU}{hr} \cdot \frac{6.585 \times 10^{21} eV}{BTU} \cdot \frac{1\ mol}{6.022 \times 10^{23} molecules} \quad [46]$$

$$= \frac{0.018\ mol\ H_2}{hr}$$

$$\dot{n}_g^r = 0.0024 \frac{molecules\ H_2}{100\ eV} \cdot 30{,}000 \frac{BTU}{hr} \cdot \frac{6.585 \times 10^{21} eV}{BTU} \cdot \frac{1\ mol}{6.022 \times 10^{23} molecules} \quad [47]$$

$$= \frac{0.008\ mol\ H_2}{hr}$$

Following the calculation of $\dot{n}_f^r$ and $\dot{n}_g^r$, the effective hydrogen composition due to radiolysis, $y_{H_2}^r$, may be estimated by inserting the appropriate values into Equation [2], as shown below in Equation [48].

$$y_{H_2}^r = \frac{0.107 + 0.018 + 0.008}{0.759 + 0.018 + 0.008} = 0.169 \quad [48]$$

As expected, the predicted hydrogen composition due to radiolysis of formate and glycolate is higher than that expected from salt solution radiolysis. This is due to the assumption that the only gaseous product from formate and glycolate radiolysis is hydrogen. Note that while consideration of oxygen depletion is possible at this stage in the calculation, it is not shown here.

3.3.3 Glycolate Thermolysis

Once formate and glycolate radiolysis have been considered, it is possible to estimate the effects of glycolate thermolysis on hydrogen composition by first calculating the expected hydrogen composition of glycolate thermolytic gas products, as described in Equation [49].

$$y_g^t = 189.161 e^{\frac{-2431.9}{70+273.15}} = 0.158 \quad [49]$$

Next, the production rate of hydrogen gas by glycolate thermolysis must be calculated, according to Equations [50] and [51]. Equation [50] calculates the HGR for glycolate thermolysis at 70°C using the activation energy and rate determined at 120°C from Ashby.

$$HGR_{thermolysis} = 0.0004 \cdot 2 \cdot 0.5 \cdot 0.166 \cdot e^{\frac{-113{,}000}{8.314}\left[\left(\frac{1}{70+273.15}\right)-\left(\frac{1}{393.15}\right)\right]} = 4.31 \times 10^{-7} \frac{mol\ H_2}{L \cdot hr} \quad [50]$$

$$\dot{n}_{H_2}^t = 4.31 \times 10^{-7} \frac{mol\ H_2}{L \cdot hr} \cdot 10^6 L = 0.431 \frac{mol\ H_2}{hr} \quad [51]$$

Once $\dot{n}_{H_2}^t$ and y_g^t have been calculated, the rate of gas generation by glycolate thermolysis, $\dot{n}_g^t$, may be calculated by taking the ratio of the two quantities, as shown in Equation [52].

$$\dot{n}_g^t = \frac{\dot{n}_{H_2}^t}{y_g^t} = \frac{0.431}{0.158} = 2.728 \frac{mol}{hr} \quad [52]$$

The estimated hydrogen composition may then be modified to include glycolate thermolytic contributions, $y_{H_2}^{org}$ as shown in Equation [53]. Note that this calculation does not at this stage consider oxygen depletion. This consideration is given in Section 3.3.4.

$$y_{H_2}^{org} = \frac{0.107 + 0.018 + 0.008 + 0.431}{0.759 + 0.018 + 0.008 + 2.728} = 0.160 \quad [53]$$

It is interesting to note that added consideration of glycolate thermolysis appears to reduce the mole fraction of hydrogen in trapped gas bubbles (0.160 vs. 0.169). This is due to the relatively large formation of additional gases (N_2, N_2O, etc.) formed by glycolate thermolysis, which inherently lower the composition of hydrogen gas.

3.3.4 Oxygen Depletion

Finally, the effect of oxygen depletion by organics may be estimated by evaluating the rates of H_2 production by organics ($\dot{n}_{H_2}^{org}$) and O_2 production by salt solution radiolysis ($\dot{n}_{O_2}$), as described in Section 3.2.3. These evaluations are shown in Equations [54] and [55].

$$\dot{n}_{H_2}^{org} = 0.018 + 0.008 + 0.431 = 0.457 \frac{mol\ H_2}{hr} \quad [54]$$

$$\dot{n}_{O_2} = (1 - 0.141) \cdot 0.759 = 0.652 \frac{mol\ O_2}{hr} \quad [55]$$

It is clear that the rate of hydrogen production by organics is smaller than that of oxygen production by salt solution radiolysis (0.457 mol/hr vs. 0.652 mol/hr). Therefore, the rate of oxygen depletion, $\dot{n}_{OD}$, may be estimated as equal to $\dot{n}_{H_2}^{org}$ in the case of this example. This substitution allows for the final calculation of H_{mix} according to Equation [56].

$$H_{mix} = \frac{0.107 + 0.018 + 0.008 + 0.431}{0.759 + 0.018 + 0.008 + 2.728 - 0.457} = 0.184 \quad [56]$$

As expected, the estimation of oxygen depletion effects causes an increase in hydrogen composition, yielding an H_{mix} of 0.184 with consideration of oxygen depletion vs. the lower H_{mix} value of 0.160 without consideration of oxygen depletion. This is in agreement with the notion that O_2 from trapped gas bubbles is selectively removed by organics, leaving less total gas at a higher composition of H_2.

4.0 Conclusions

A number of conclusions may be made about the models presented within this report. First, a selection of improved fits have been employed to describe the effect of nitrate and nitrite on the hydrogen composition in gases generated by salt solution radiolysis. An exponential fit has been recommended to describe observed behavior in nitrite solutions, while an inverse linear fit has been recommended to describe observed behavior in nitrate solutions.

Second, the mechanism for hydrogen production by formate and glycolate radiolysis described by Crawford and King has been incorporated into the bubble composition model in order to account for organic radiolytic effects on hydrogen composition. This was done by assuming that the only gaseous product of organic radiolysis is H_2, which is a conservative assumption.

Third, the rate of hydrogen generation by glycolate thermolysis suggested by Crawford and King has been incorporated by evaluation of offgas composition data reported by Ashby. It was noted that the temperature dependence of glycolate thermolytic offgas composition allows for decreases in predicted hydrogen composition.

Finally, a conservative estimation of the rate of oxygen depletion by formate and glycolate has been incorporated by evaluation of the rate of hydrogen generated by formate and glycolate degradation against the rate of oxygen generation by salt solution radiolysis. It has been found that this complete model predicts values of hydrogen composition higher than is predicted by salt solution radiolysis alone (0.184 vs. 0.141), which agrees with the observation that organics tend to increase the concentration of hydrogen in trapped gas bubble vapors. Both of these values are lower than the original H_{mix} calculated by Hester for water radiolysis using the same nitrate and nitrite concentrations (0.20).

5.0 Recommendations

It is recommended that testing with radioactive waste be conducted to evaluate the accuracy of the calculation method described in this report. Testing should evaluate the generation rates of H_2, N_2, N_2O, and any other possible gases (CO, CO_2, NO, etc.) formed from treatment of radioactive waste in caustic conditions as a function of temperature. The performance of this testing may be enhanced with the use of an inert carrier gas (e.g. Kr or Ar) such that small changes in N_2 and O_2 generation rates may be detected.

Additional testing should be performed to examine the impact of organics other than formate and glycolate on this model. Focus should be given to understanding the composition of radiolytic and thermolytic offgas as a function of temperature and organic molecule speciation and concentration. Such data may be coupled with the organic hydrogen generation rate model proposed by Hu[3] in order to develop a comprehensive hydrogen bubble composition model capable of describing the effects of multiple organic species.

6.0 References

1. C.L. Crawford, W.D. King, "Impacts of Glycolate and Formate Radiolysis and Thermolysis on Hydrogen Generation Rate Calculations for the Savannah River Site Tank Farm," Savannah River National Laboratory, SRNL-STI-2017-00303, Rev. 0, 2017.
2. E.C. Ashby, A. Annis, E.K. Barefield, D. Boatright, F. Doctorovich, C.L. Liotta, H.M. Neumann, A. Konda, C.F. Yao, K. Zhang, N.G. McDuffie, "Synthetic Waste Chemical Mechanism Studies," Westinghouse Hanford Company, WHC-EP-0823, 1994.
3. T.A. Hu, "Empirical Rate Equation Model and Rate Calculations of Hydrogen Generation for Hanford Tank Waste," HNF-3851, Rev. 1, 2004.
4. S.T. Isom, "Evaluation of Glycolate Impact to Tank Farm and Radiolytic Hydrogen Generation," Savannah River Remediation, X-TTR-S-00060, Rev. 1, 2017.
5. C.L. Crawford, C.J. Martino, J.I. Mickalonis, "Task Technical and Quality Assurance Plan for Glycolate Impacts on Savannah River Site Tank Farm Hydrogen Generation and Corrosion," Savannah River National Laboratory, SRNL-RP-2017-00082, Rev. 1, 2017.
6. W.A. Condon, "Potentially Inadequate Recognition of the Effect of Organics on Hydrogen Generation Rates in CSTF," Savannah River Remediation, PI-2017-0003, 2017.
7. K.M. Brotherton, "Potentially Inadequate Recognition of the Effect of Organics on Hydrogen Gas Generation Rates in DWPF Process Vessels," Savannah River Remediation, PI-2017-0004, 2017.
8. A.V. Staub, "Potentially Inadequate Recognition of the Effect of Organics on Hydrogen Generation Rates in Saltstone," Savannah River Remediation, PI-2017-0002, 2017.
9. J.R. Zamecnik, Edwards, T.B., "Defense Waste Processing Facility Nitric-Glycolic Flowsheet Chemical Process Cell Chemistry: Part 2," Savannah River National Laboratory, SRNL-STI-2017-00172, Rev. 0, 2017.
10. C.J. Martino, "Analysis of Tank 38H (HTF-38-11-69,70) and Tank 43H (HTF-43-11-71,72) Samples for Support of the Enrichment Control and Corrosion Control Programs," Savannah River National Laboratory, SRNL-L3100-2011-00147, Rev. 0, 2011.
11. D.C. Koopman, D.R. Best, B.R. Pickenheim, "SRAT Chemistry and Acid Consumption During Simulated DWPF Melter Feed Preparation," Savannah River National Laboratory, WSRC-STI-2008-00131, Rev. 0, 2008.
12. J.R. Hester, "Radiolytic Bubble Gas Hydrogen Compositions," Westinghouse Savannah River Company, WSRC-TR-2001-00193, Rev. 1, 2002.
13. C.H. Keilers, "Flammable Gas Generation Mechanisms for High Level Liquid Waste Facilities," Savannah River Remediation, X-ESR-G-00062, Rev. 1, 2017.
14. C.S. Boley, "G-Value Prediction for Hydrogen Generation Rates for High Level Waste (U)," Westinghouse Savannah River Company, X-CLC-H-00100, Rev. 0, 1998.
15. N.E. Bibler, J.M. Pareizs, T.L. Fellinger, C.J. Bannochie, "Measurement and Prediction of Radiolytic Hydrogen Production in Defense Waste Processing Slurries at Savannah River Site," Savannah River National Laboratory, WSRC-STI-2006-00114, Rev. 1, 2006.
16. R.F. Bradley, "Radiolysis of Liquid Waste During Bedrock Storage," Savannah River Laboratory, DP-1264, 1971.
17. R.A. Peterson, "Hydrogen Release from Simulated Sludge and Saltcake," Savannah River Technology Center, WSRC-TR-98-00341, Rev. 0, 1998.
18. "Technical Reviews," Savannah River Site, Manual E7, Procedure 2.60, Rev. 17, 2016.
19. "Savannah River National Laboratory Technical Report Design Checklist," Savannah River Site, WSRC-IM-2002-00011, Rev. 2, 2004.
20. H.A. Mahlman, "The OH Yield in the Co-60 γ-Radiolysis of HNO_3," *Journal of Chemical Physics,* 35 [3] (1961).
21. R.A. Peterson, C.L. Crawford, "Hydrogen Production from Radiolysis of Sludge Systems," Savannah River Technology Center, WSRC-TR-98-00452, Rev. 0, 1998.

22. "Bedrock Waste Storage - Technical Progress Report (February-April 1972)," Savannah River Laboratory, DPST-72-122-2, 1972.
23. D.D. Walker, “Organic Compounds in Savannah River Site High-Level Waste,” Savannah River Technology Center, WSRC-TR-2002-00391, Rev. 0, 2002.

Distribution:

timothy.brown@srnl.doe.gov
michael.cercy@srnl.doe.gov
alex.cozzi@srnl.doe.gov
david.crowley@srnl.doe.gov
David.Dooley@srnl.doe.gov
a.fellinger@srnl.doe.gov
samuel.fink@srnl.doe.gov
erich.hansen@srnl.doe.gov
connie.herman@srnl.doe.gov
david.herman@srnl.doe.gov
Elizabeth.Hoffman@srnl.doe.gov
Kevin.Kostelnik@srs.gov
Kevin.Fox@srnl.doe.gov
john.mayer@srnl.doe.gov
daniel.mccabe@srnl.doe.gov
thelesia.oliver@srnl.doe.gov
frank.pennebaker@srnl.doe.gov
William.Ramsey@SRNL.DOE.gov
luke.reid@srnl.doe.gov
geoffrey.smoland@srnl.doe.gov
michael.stone@srnl.doe.gov
Boyd.Wiedenman@srnl.doe.gov
bill.wilmarth@srnl.doe.gov
Records Administration (EDWS)
jeffrey.crenshaw@srs.gov
james.folk@srs.gov
roberto.gonzalez@srs.gov
patrick.jackson@srs.gov
tony.polk@srs.gov
jean.ridley@srs.gov
patricia.suggs@srs.gov
Kevin.Brotherton@srs.gov
Richard.Edwards@srs.gov
terri.fellinger@srs.gov
eric.freed@srs.gov
jeffrey.gillam@srs.gov
barbara.hamm@srs.gov
bill.holtzscheiter@srs.gov
john.iaukea@srs.gov
Vijay.Jain@srs.gov
Victoria.Kmiec@srs.gov
chris.martino@srnl.doe.gov
jeff.ray@srs.gov
paul.ryan@srs.gov
Azadeh.Samadi-Dezfouli@srs.gov
hasmukh.shah@srs.gov
aaron.staub@srs.gov
Austin.Chandler@srs.gov
Steven.Simner@srs.gov
celia.aponte@srs.gov
timothy.baughman@srs.gov
earl.brass@srs.gov
Thomas.Huff@srs.gov
ryan.mcnew@srs.gov
n-rao.pasala@srs.gov
john.schwenker@srs.gov
Christie.sudduth@srs.gov
arthur.wiggins@srs.gov
Maria.Rios-Armstrong@srs.gov
Rachel.Seeley@srs.gov
Lauryn.Jamison@srs.gov
Spencer.Isom@srs.gov
Christine.Ridgeway@srs.gov
Mason.Clark@srs.gov
Thomas.colleran@srs.gov
hilary.bui@srs.gov